parameters derived from the long period and horizontal components of seismic data.

1. Rumelhart, D. E., Hinton, G. E. and Williams, R. J., *Parallel Distributed Processing: Explorations in the Microstructure of Cognition. Vol 1: Foundations* (eds Rumelhart, D. E. and McClelland, J. L.), MIT, Cambridge, 1986, pp. 318–362.
2. Kosko, B., *Neural Networks and Fuzzy Systems – A Dynamical Systems Approach to Machine Intelligence*, Prentice Hall, Englewood Cliffs, NJ, 1992.
3. Zuruda, J. M., *Introduction to Artificial Neural Systems*, West Publishing Co., NY, 1992.
4. Rumelhart, D. E., Hinton, G. E. and Williams, R. J., *Nature*, 1986, **323**, 9.
5. Ulrych, T. J. and Bishop, T. N., *Rev. Geophys. Space Phys.*, 1975, **13**, 183–200.
6. Ulrych, T. J. and Clayton, R. W., *Phys. Earth Planet. Inter.*, 1976, **12**, 188–200.
7. Nair, G. J., *Phys. Earth Planet. Inter.*, 1983, **32**, 36–44.
8. Roy, F., Report No. BARC/1341, 1986.
9. Mowat, W. M. H. and Burch, R. F., Reference No. AWRE/44/47/29, AWRE, Aldermaston, 1974.
10. Varghese, T. G., Roy, F., Rao, B. S. S., Suryavanshi, M. P. and Bharthur, R. N., *Phys. Earth. Planet. Int.*, 1979, **18**, 87–94.
11. Arora, S. K., Report No. BARC/309, 1967.
12. Roy, F. and Basu, T. K., Report No. BARC/E/017, 1994.
13. Murty, G. S., Nair, G. J. and Roy, F., *Mausam*, 1979, **30**, 337–341.
14. Roy, F., *J. Biomed. Eng. Soc. India*, 1990, **12**, 1–10.
15. Roy, F., *Bull. Seismol. Soc. Am.*, 1984, **74**, 1623–1643.
16. Roy, F., Arora, S. K. and Basu, T. K., *Phys. Earth Planet Int.*, 1992, **73**, 264–273.
17. Dahlman, O. and Israelson, H., *Monitoring Underground Nuclear Explosions*, Elsevier, Amsterdam, 1977.
18. Pomeroy, P. W., Best, W. J. and McEvilly, T. V., *Bull. Seismol. Soc. Am.*, 1982, **72**, S89–S129.
19. Kelly, E. J., MIT, Lincoln Lab., Tech. Note 1968-8, 1968.
20. Weichert, D. H., *Z. Geophys.*, 1971, **37**, 147–152.
21. Basu, T. K. and Arora, S. K., Report No. BARC/1348, 1987.
22. Roy, F., Report No. BARC/1475, 1989.

ACKNOWLEDGEMENTS. I am grateful to Dr S. K. Sikka for his encouragement and interest in this work. I thank Dr S. K. Arora for giving some useful suggestions. I also express thanks to Shri R. N. Bharthur, Shri A. G. V. Prasad and Shri E. Unnikrishnan for their help in providing transcripts of digital data of seismograms used in this work.

Received 15 July 1997; revised accepted 31 October 1997

RESEARCH COMMUNICATIONS

X-ray contact microscopic imaging in keV spectral region using laser-produced plasmas

J. A. Chakera†, P. D. Gupta, Yu. Geondgian*, V. V. Sorokin*, V. Yu. Korol* and V. P. Avtonomov*

Centre for Advanced Technology, P.O. CAT, Indore 452 013, India
*P.N. Lebedev Physical Institute, Russian Academy of Sciences, Moscow, Russia

We report here contact microscopic imaging in keV spectral region using pulsed X-ray emission from laser-produced plasmas. The X-ray source was produced by focusing single laser pulses of second harmonic of Nd : glass laser with a peak power of 3 GW in 3 nS (FWHM) on planar targets of copper. Single shot X-ray images of 1 : 1 magnification and an estimated spatial resolution ~ 120 nm were obtained on a ERP-40 photoresist-coated silicon wafer. These images were subsequently viewed under scanning electron microscope and atomic force microscope for high magnification, and with a differential interference contrast optical microscope for colour contrast. Details of the imaging technique are presented, and images recorded for yeast cells are given as an example.

X-RAY contact microscopy has recently drawn considerable attention for imaging biological cells with high spatial resolution[1–3]. This is because in conventional optical microscopy, the spatial resolution is limited by the wavelength of illuminating radiation to ~ 0.5 μm. In electron microscopy, it is not possible to image biological cells in their natural living conditions due to the necessity of slicing, dehydration, and staining of the sample to obtain a good contrast. In comparison, X-ray contact imaging in the so-called water window spectral region (from 2.3 nm to 4.4 nm corresponding to K-absorption edges of oxygen and carbon respectively) can provide high contrast images in presence of water. Many authors[1–7] have reported on X-ray contact microscopic imaging of biological samples using X-rays in this spectral region.

An important potential application of X-ray microscopic imaging can be in elemental mapping of a sample[1,3]. The idea is based on difference imaging of the sample using X-rays in two different spectral regions on either side of an absorption edge of an element in the sample under investigation. However, since K and L absorption edges of many elements of interest occur at $\lambda < 1$ nm, one has to use an X-ray source in keV spectral region. Moreover, a large variety of biological cells have a size of several microns, in which case X-rays in the water-window spectral region would be strongly attenuated[3]. Thus, X-ray microscopic imaging using radiation of $\lambda < 1$ nm can be of considerable practical interest. However, much less attention has been paid to X-ray contact microscopic imaging in this spectral range.

†For correspondence.

In this paper, we describe the use of a laser-produced plasma X-ray source for X-ray contact microscopic imaging in keV spectral region. Single shot, high resolution images of yeast cells are obtained with unit magnification on a ERP-40 photoresist-coated silicon wafer using X-ray emission from a copper plasma. Analysis of these images performed using a scanning electron microscope (SEM) and an atomic force microscope (AFM) shows sufficient contrast and features which are not observed when the sample is viewed directly under an optical microscope. Spatial resolution is estimated to be ~110 to 130 nm for 5 μm thick samples. Further, height profile of the developed photoresist obtained from AFM analysis provides a two-dimensional map of integrated X-ray absorption of the sample. This can be of interest for stereoscopic imaging application as a potential technique for elemental mapping of biological objects.

The basic idea underlying the contact imaging technique is to record a contact shadowgram of a sample placed on a photoresist-coated silicon wafer by exposing it to a short duration burst of radiation from a point X-ray source (Figure 1). After exposure, the latent image of unit magnification in the photoresist is chemically developed to yield a relief pattern which corresponds to a two-dimensional topographical map of integrated X-ray attenuation of the original sample. A spatial resolution of the image of the order of 100 nm can be achieved which is mainly governed by diffraction[7,8] of the X-ray radiation from the sample and penumbral blurring[7] of the image due to finite X-ray source size and sample thickness. High magnification of the image is accomplished in the viewing stage of the developed photoresist. The image can be seen with high magnification under either an SEM or an AFM, while essentially maintaining the spatial resolution achieved in the recording stage.

An important feature of this imaging technique lies in the height profile of the developed photoresist. This is because when the exposed photoresist is developed, the etching depth at a given point depends on the X-ray dose received by that point. One thus gets a height profile in the developed photoresist (Figure 2) which represents a two-dimensional map of the thickness integrated X-ray attenuation of the sample. A quantitative map of the height profile of the photoresist can be obtained from the AFM analysis. Alternatively, one can view the X-ray image under a differential interference contrast (DIC) optical microscope. Interference of light reflected from the top and bottom interfaces of the developed photoresist would result in a colour pattern governed by the height profile, However, in this case, the spatial resolution of the magnified image will be limited by the wavelength of the visible light.

Experiments were performed using D2ML Nd : glass laser system at P. N. Lebedev Institute. Soft X-ray source was produced by irradiating planar foils of copper with single laser pulses of energy ~9 J in 3 nS (FWHM) at the second harmonic ($\lambda = 0.53$ μm) of Nd : glass laser. A schematic diagram of the experimental set up is shown in Figure 3. A plano-convex lens of 120 mm focal length focused the laser beam on the target to a focal spot diameter of ~80 μm. Laser intensity for these irradiation conditions was estimated to be ~ 6×10^{13} W/cm^2. The target chamber was evacuated to 10^{-2} torr and the target was moved after each laser shot to provide fresh surface for plasma production.

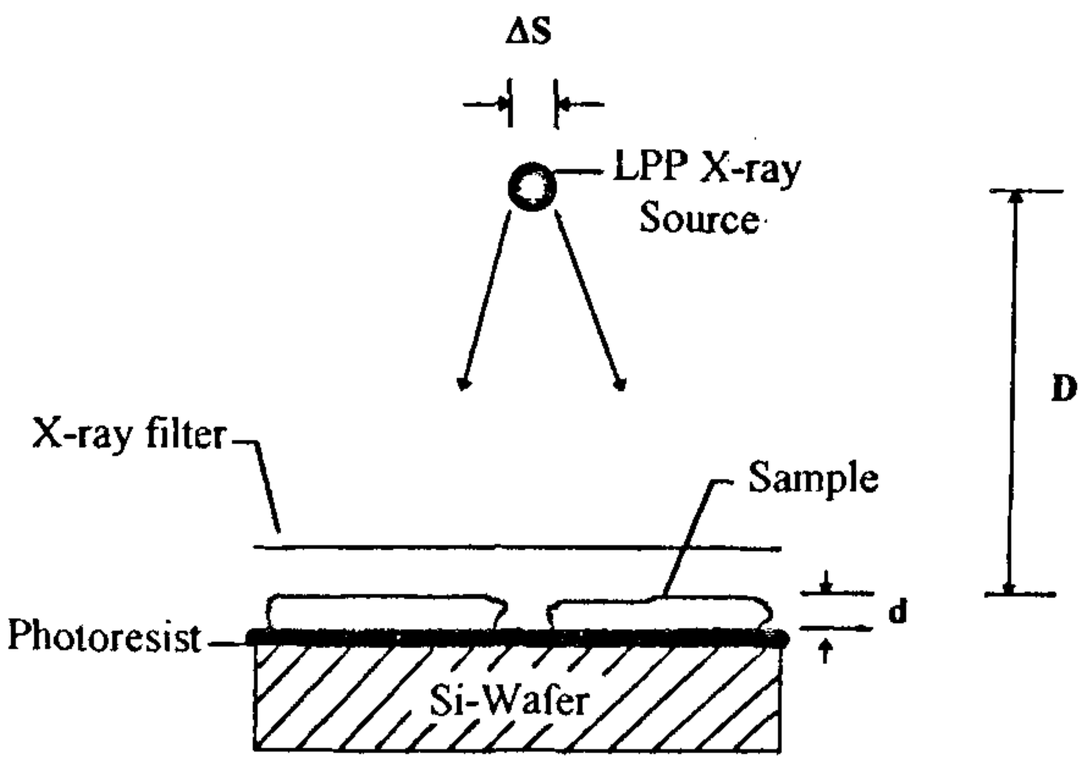

Figure 1. X-ray contact imaging technique.

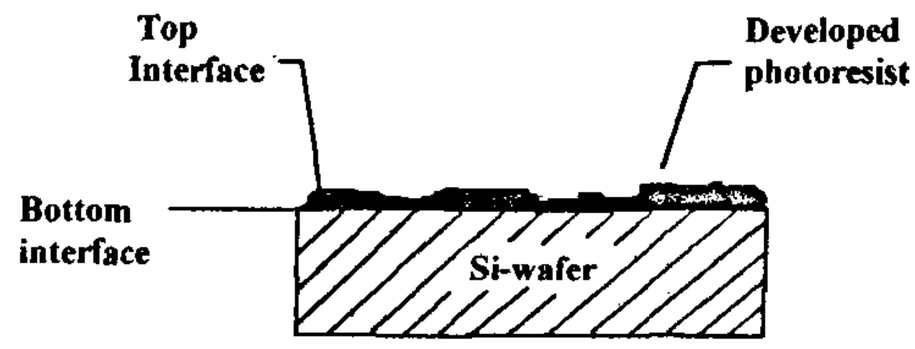

Figure 2. A typical height profile of the developed photoresist.

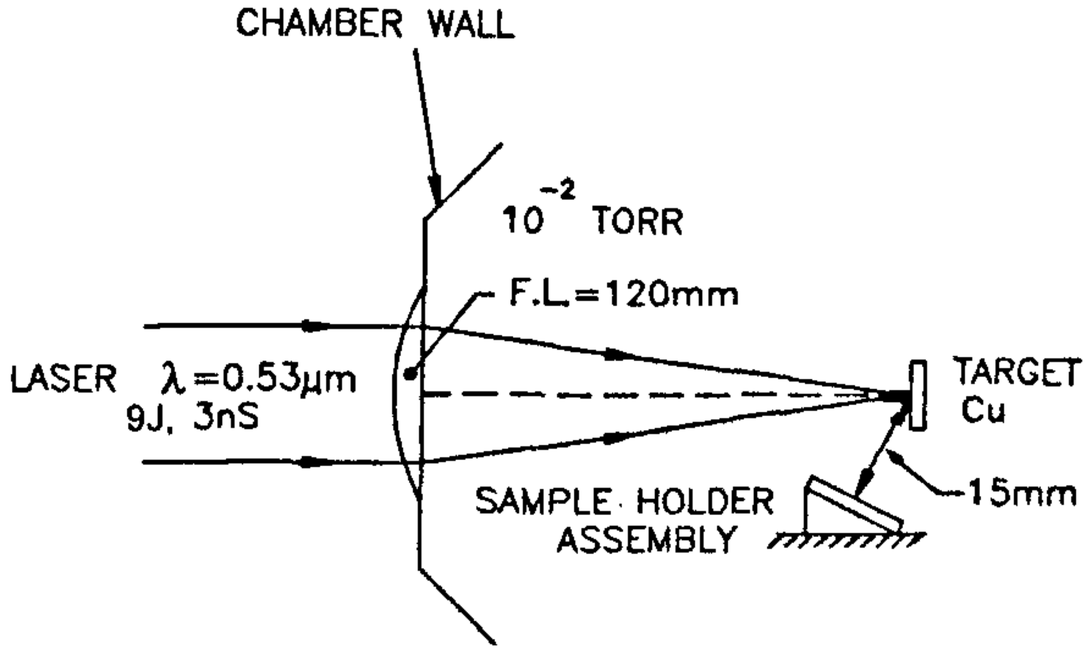

Figure 3. Experimental setup of laser-produced plasma X-ray source.

Biological samples, viz. yeast cells were placed on a thin nitrocellulose film of 100 nm thickness stretched on a fine copper grid of 70 μm mesh size and the same was kept in contact with a photoresist-coated silicon wafer. A schematic of the sample holder assembly is shown in Figure 4. The silicon wafer had a 0.8 μm thick coating of ERP-40 photoresist[9] baked to 100°C for a period of one hour. The minimum X-ray dose required for this photoresist is ~ 2 mJ/cm^2. A polythene foil of 1.2 μm thickness was placed between the X-ray source and the sample to serve as an X-ray filter and to prevent plasma debris of the target from hitting the sample. This foil had a cut-off energy (defined as the photon energy for which transmission through the foil reduces to 1/e of the input intensity) of $h\nu \sim 0.8$ keV. The sample holder assembly was placed at a distance of 15 mm from the target and oriented at an angle of 70° with the target normal. This distance was kept sufficiently large so that the polythene foil is not damaged by the plasma blow-off from the target.

X-ray emission spectrum of the copper plasma was measured using a KAP crystal in Bragg reflection geometry. The spectrum showed intense emission features in the wavelength region of ~ 0.8 nm to 1.1 nm (photon energy range $h\nu \sim 1.1$ keV to 1.5 keV) due to the line and free-bound recombination transitions in L shell of Cu ions. A single shot X-ray dose of ~ 10 mJ/cm^2 incident on the sample was quite appropriate for exposure of the ERP-40 photoresist. Attenuation of X-ray dose in the sample is governed by its thickness and composition. For a 5 μm thick protein layer[7], the attenuation for X-rays of $\lambda \sim 1$ nm is estimated to be ~ 3. The X-ray dose distribution on the surface of the resist is therefore ensured to be within the dynamic range of the resist. Moreover, since a 0.8 μm thick ERP-40 resist absorbs only ~ 10% of the X-ray radiation in the above spectral range, a homogeneous energy deposition would occur along the thickness of the resist layer.

Exposed photoresist samples were developed in a 1 : 3 mixture of ethyl methyl ketone and propanol for 8 min. The developer concentration and development time were chosen so that a negligible dissolution of unexposed resist areas occur during the development process. Resist contrast coefficient γ (slope of the curve showing normalized remaining thickness of the resist versus log exposure) was ~ 0.9. The developed photoresist samples were analysed under SEM, AFM and DIC optical microscope. Resist samples were gold sputter-coated for SEM analysis.

Figure 5 shows an SEM picture of the image of the yeast cells in the developed photoresist at a magnification of 3000 ×. These pictures were taken at low accelerating voltages as the photoresist is very electron-sensitive even when sputter-coated. The sample consisted of yeast cells of ~ 5 μm diameter and ~ 30 μm length dimensions. The tubular structure of these cells is clearly seen in the picture. Also seen are the internal structures of ~ 2–3 μm size representing regions of higher optical density for the exposed X-ray spectrum. This can be compared with the yeast cells as viewed under a conventional optical microscope (Figure 6). It may be noted that direct viewing of the sample by optical microscope does not reveal internal structure details due to very

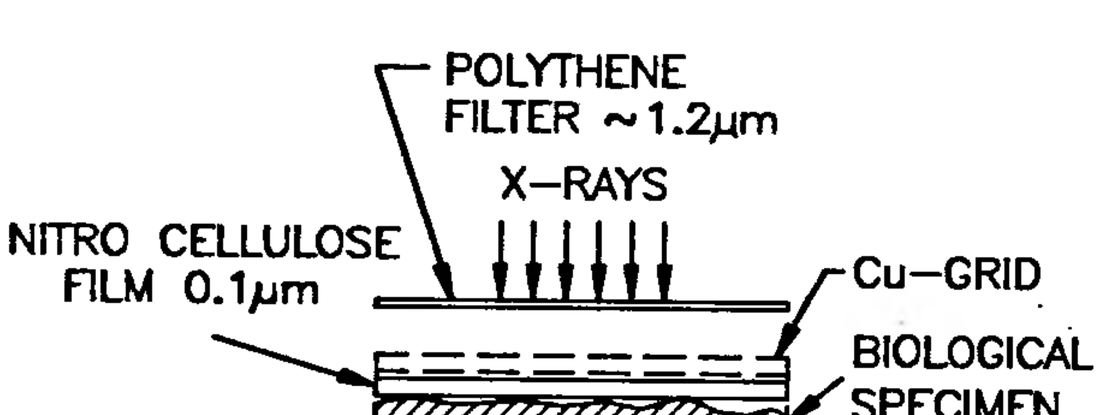

Figure 4. Schematic of sample holder assembly.

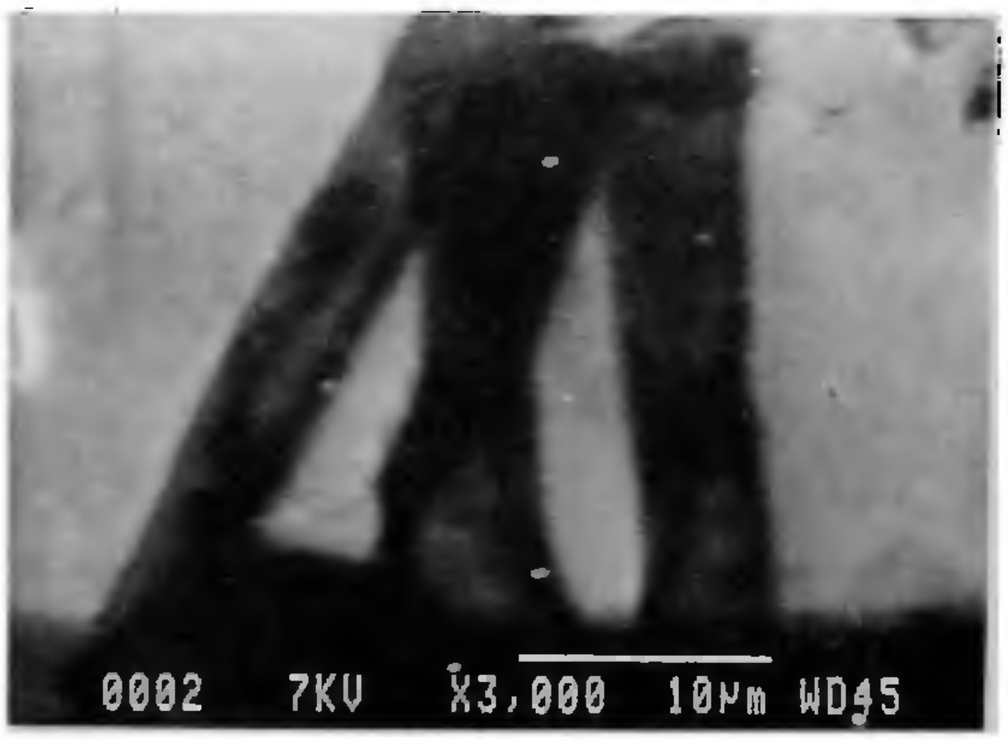

Figure 5. X-ray contact image of yeast cells as seen under SEM.

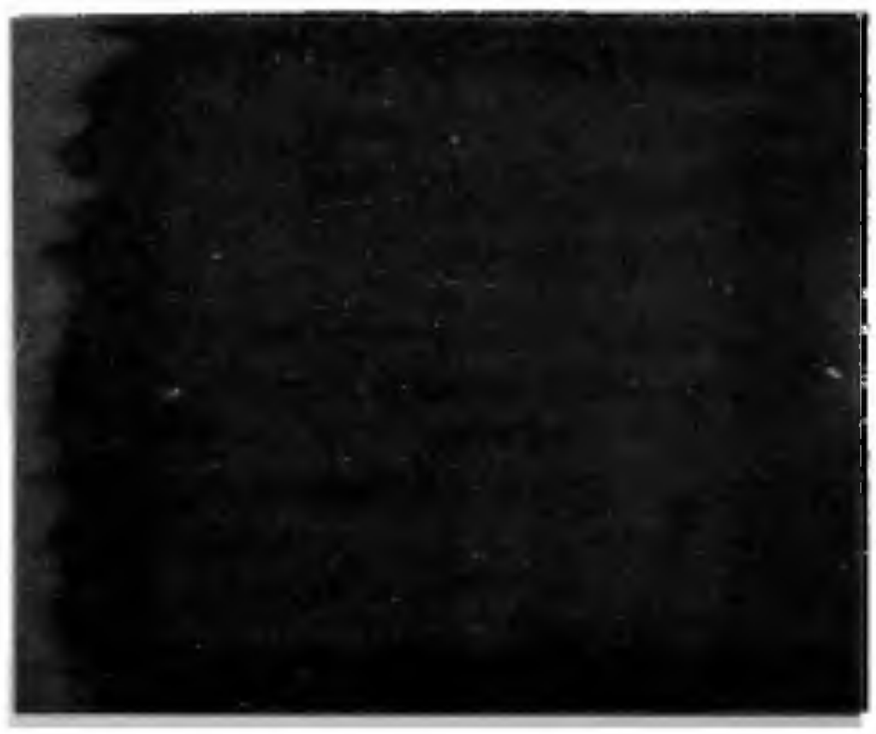

Figure 6. Yeast cells seen under optical microscope.

low contrast of the sample in the visible optical region.

Figure 7 shows X-ray image of the yeast cells observed under a DIC optical microscope. This image shows quite distinctly both boundaries and internal structure of the cells. Different colours represent regions of different X-ray attenuation in the sample as discussed earlier. The outer rectangular boundary in this figure is of the 70 μm mesh used. The colour difference of the cell boundary and internal regions is caused by difference in their X-ray absorption properties.

Next, an AFM picture of the photoresist image of the yeast cells is shown in Figure 8. Height profile distribution in the developed photoresist is also depicted on a scale. This picture thus represents a two-dimensional map of the height profile of the developed photoresist. This can be used to find out the X-ray dose distribution on the exposed surface of the resist and thereby the distribution of optical density of the sample in the X-ray spectral region. Taking into consideration the symmetrical form of yeast cells, it can be inferred that the internal structures seen in the picture are regions of higher X-ray attenuation than those of the surrounding regions. A detailed quantitative information would necessitate different X-ray spectral ranges for taking such shadowgrams. Nevertheless, the important role of keV X-ray shadowgraphy is clearly evident from the observed contrast and features in the images which are not revealed when the sample is viewed directly under an optical microscope.

Spatial resolution in the contact imaging technique is governed by X-ray diffraction from the sample and penumbral blurring of the image due to finite source size (Figure 1). If a sample of thickness d is illuminated by X-rays of wavelength λ, Fresnel diffraction would limit the resolution[7,8] Δx_1 to $\sim (\lambda d)^{1/2}$. For an X-ray wavelength of ~ 1 nm and a sample thickness of 5 μm, this limit would come to ~ 70 nm. Next, the penumbral blurring of the image Δx_2, for a source of size ΔS kept at a distance D from the sample, is given by $\Delta S \cdot d/D$. For the X-ray source size of laser-produced plasma of ~ 80 μm and the source to sample separation of ~ 15 mm, the penumbral blurring of the image for a sample of 5 μm thickness is ~ 30 nm. Thus the overall spatial resolution limit due to the combined effect of diffraction and geometry, $(\Delta x_1^2 + \Delta x_2^2)^{1/2}$, would be ~ 80 nm. However, practical spatial resolution would be worse than this limiting value because of the resolution limit due to statistical noise of photons absorbed in the photoresist[3,7] and the resolution of the photoresist itself. Resolution of the ERP-40 resist[9] at $\lambda = 1$ nm, is ~ 10 nm, and is thus not a serious contributor in the present case. However, for any X-ray microscopic imaging, statistical noise of photons would limit the resolution. For a single shot exposure of 10 mJ/cm^2, this value is estimated[3] to be in the range of 30 to 50 nm. Thus a spatial resolution of ~ 110–130 nm is expected for the imaging parameters involved.

An experimental measurement of spatial resolution can be made from the images of well-defined physical microstructures recorded in the same manner. A spatial resolution of 195 nm was observed from the edge profile of a copper grid bar of 10 μm thickness kept in direct contact with the photoresist and exposed to X-ray emission from a laser-produced copper plasma[10]. This higher value is quite understandable because the available copper grid was of a higher thickness of 10 μm (compared to the yeast cells) for which both the diffraction and penumbral blurring would be larger. In view of this, the estimated spatial resolution for the yeast sample is consistent with the experimentally observed value for the copper grid structure.

Pulsed X-ray emission from laser-produced plasma is well suited for achieving high spatial resolution in contact imaging. Although synchrotron radiation source

Figure 7. Colour contrast observed from X-ray image of yeast cells as viewed under an optical DIC microscope.

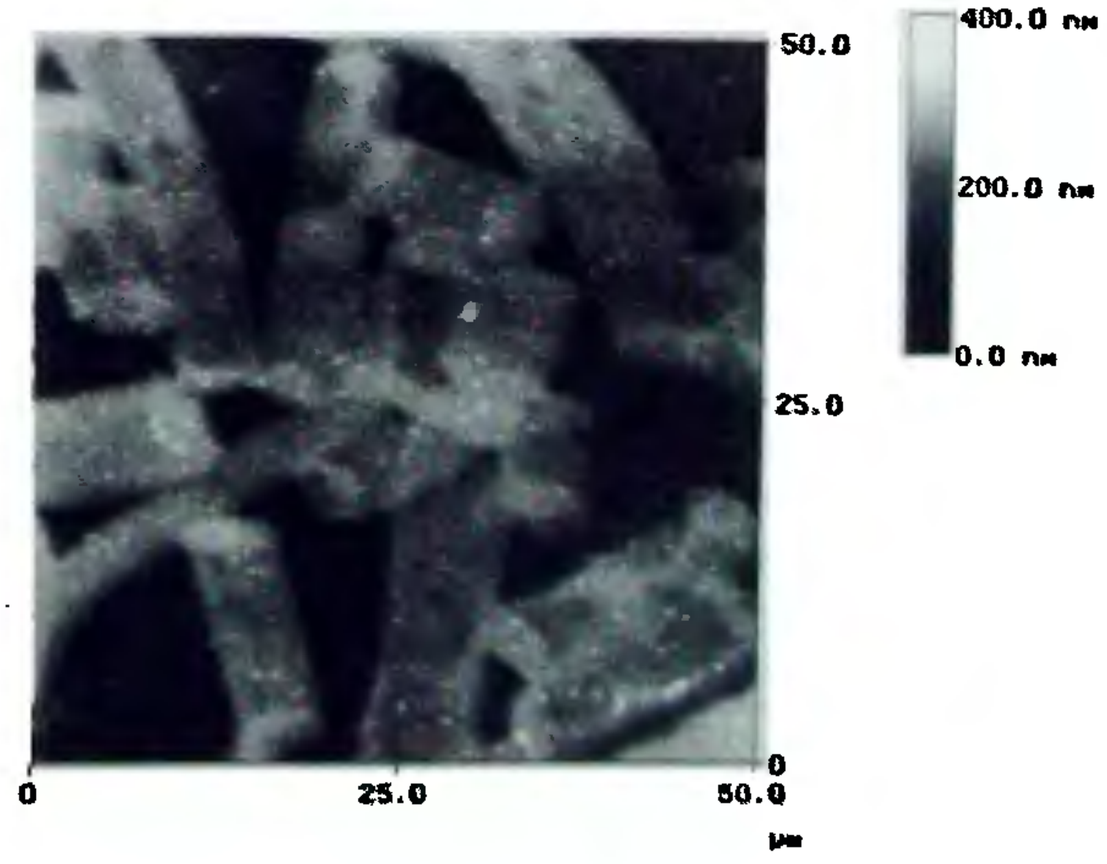

Figure 8. X-ray contact image of yeast cells showing height profile of the developed photoresist as observed under an AFM.

provides an excellent coverage in X-ray spectral region, an exposure of an order of millisecond is usually required to achieve the necessary dose. This may result in degradation of spatial resolution on account of thermal vibrations in the sample or blurring caused by expansion of the sample due to heating during the long exposure period[1,2]. Laser-produced plasmas, on account of their high peak brightness, can provide sufficient exposure in a single pulse of short duration (few nanoseconds or smaller), thereby avoiding the above problems. Further, smaller size and much lower capital cost of a laser-produced plasma source are obvious advantages for a moderate size laboratory.

In conclusion, X-ray contact microscopic imaging is performed in keV X-ray spectral region using a laser-produced plasma X-ray source. Images of unit magnification are obtained for ~5 μm thick yeast cells in single shot exposures of ~10 mJ/cm^2 with an estimated spatial resolution of ~120 nm. These images are observed with high magnification under a scanning electron microscope and an atomic force microscope. X-ray images show internal structures which are not seen under a conventional optical microscope due to low contrast in the visible region. Height profile of the developed photoresist observed under AFM correspond to a two-dimensional map of thickness integrated X-ray attenuation of the sample. This can be useful for potential application of elemental mapping of biological objects.

1. Richardson, M., Shinohara, K., Tanaka, K. A., Kinjo, Y., Ikeda, N. and Kado, M., *Soc. Photo-Opt. Instrum. Eng.*, 1992, **1741**, 133–141.
2. Stead, A. D., Cotton, R. A., Duckett, J. G., Goode, J. A., Page, A. M. and Ford, T. W., *J. X-ray Sci. Technol.*, 1995, **5**, 52–64.
3. Tomie, T., Shimizu, H., Majima, T., Kanayama, T., Yamada, M. and Miura, E., *Soc. Photo-Opt. Instrum. Eng.*, 1992, **1741**, 118–128.
4. Bollanti, S., Lazzaro, P. D., Flora, F., Giordano, G., Letardi, T., Schina, G., Zheng, C. E., Filippi, L., Palladino, L., Reale, A., Taglieri, G., Batani, D., Mauri, A., Belli, M., Scafati, A., Reale, L., Albertano, P., Grilli, A., Faenov, A., Pikuz, T. and Cotton, R., *J. X-ray Sci. Technol.*, 1995, **5**, 261–277.
5. Tomie, T., Shimizu, H., Majima, T., Yamada, M., Kanayama, T., Kondo, H., Yano, M. and Ono, M., *Science*, 1991, **252**, 691–693.
6. Eason, R. W., Cheng, P. C., Feder, R., Michette, A. G., Rosser, R. J., O'Neill, F., Owadano, Y., Rumsby, P. T., Shaw, M. J. and Turcu, I. C. E., *Opt. Acta*, 1986, **33**, 501–516.
7. Fletcher, J., Cotton, R. and Webb, C., *Soc. Photo-Opt. Instrum. Eng.*, 1992, **1741**, 142–153.
8. Bijkerk, F., Louis, E., Vander Wiel, M. J., Turcu, E. C. I., Tallents, G. J. and Batani, D., *J. X-ray Sci. Technol.*, 1992, **3**, 133–151.
9. Avtonomov, V. P., Vragov, K. M., Duda, V. I., Geondgian, Yu. G., Korol, V. Yu., Kuznecov, V. Ya. and Sorokin, V. V., *FIAN reprint*, 1991, No. 38, Moscow.
10. Chakera, J. A., Kumbhare, S. R. and Gupta, P. D., Proceedings of the National Laser Symposium, Indore, India, Feb 1997, pp. 286–287.

ACKNOWLEDGEMENTS. We thank Dr D. D. Bhawalkar and Academician N. G. Bosov for their keen interest and encouragement during the course of this work. The work is performed under ILTP collaboration project supported by Department of Science and Technology, India, and Russian Academy of Sciences, Moscow, Russia.

Received 22 August 1997; revised accepted 3 December 1997

Effect of 45 MeV ^{7}Li and 68 MeV ^{16}O charged particles on the microsomal membrane fluidity

M. Srivastava, D. Choudhary, A. Sarma* and R. K. Kale†

School of Life Sciences, Jawaharlal Nehru University, New Delhi 110 067, India
*Nuclear Science Centre, New Delhi 110 067, India

Microsomes prepared from liver of male Sprague Dawley rats were irradiated with various fluences of 45 MeV ^{7}Li and 68 MeV ^{16}O charged particles. The change in fluidity and lipid peroxidation was measured in terms of fluorescence polarization and MDA formation respectively. The fluidity of membrane was found to decrease with increase in fluence of both the particle radiations and could be ascribed to peroxidative damage. This effect persisted in post-irradiation period. 68 MeV ^{16}O ions were found to be more detrimental compared to 45 MeV ^{7}Li. Since membranes are also considered to be the critical targets of radiation action, these findings may have significance in understanding the radiobiological effect of high linear energy transfer radiation.

IMPORTANCE of high linear energy transfer (LET) radiations in the cancer therapy and estimating risks, especially in the space flights, has generated lot of interest in their radiobiological studies. Extensive work has been carried out using various biological endpoints. However, very little information is available on the effect of high LET radiations on biological membranes, which apart from DNA, are considered to be the critical targets of the detrimental actions of ionizing radiations. Therefore, an attempt was made to study the effect of 45 MeV ^{7}Li and 68 MeV ^{16}O ions in microsomal membranes in terms of fluorescence polarization using 1,6-diphenyl-1,3,5-hexatriene (DPH) probe which localizes in the fatty acyl side chain region of lipid bilayer[1].

Microsomes were prepared from the liver of Sprague Dawley rats (200–250 g body weight) as described by Varshney and Kale[2]. The animals were maintained in

†For correspondence.